Available online at www.sciencedirect.com

ScienceDirect

Procedia CIRP 77 (2018) 86–89

www.elsevier.com/locate/procedia

8th CIRP Conference on High Performance Cutting (HPC 2018)

Experimental Analysis of Cutting Force Reduction During Ultrasonic Assisted Turning of Ti6Al4V

Iñigo Llanos[a]*, Ángela Campa[a], Ariane Iturbe[a], Pedro J. Arrazola[b], Oier Zelaieta[a]

[a]IK4-Ideko, Arriaga industrialdea 2, Elgoibar, 20870, Spain

[b] Faculty of Engineering, Mondragon University, Mondragón 20500, Spain

* Corresponding author. Tel.: +0034-943748000; fax: +0034-943 743 804. *E-mail address:* illanos@ideko.es

Abstract

The machining of difficult-to-cut materials involves limitations leading to low productivity in conventional machining processes due to high cutting forces and tool wear rates. The ultrasonic assisted machining techniques have been reported to reduce these drawbacks significantly, enabling the increase of productivity when machining this kind of materials. In the case of the reductions on cutting forces and their control, they can lead to important improvements concerning achievable Material Removal Rates (MRR) on processes where the maximum cutting forces are limited due to part-tool deflections or the appearance of chatter vibrations. The present study analyses the cutting force reductions generated when ultrasonically assisted turning of Ti6Al4V. The obtained results were analyzed for identifying the most relevant parameters generating such force reductions. Finally, an empirical model was developed allowing the calculation of the cutting forces to be generated during ultrasonic assisted turning operations of Ti6Al4V.

Keywords: Ultrasonic assisted turning; Cutting force reduction; Empirical modelling; Ti6Al4V

1. Introduction

The ultrasonic Assisted Turning (UAT) process has been reported to provide several advantages in comparison to conventional turning. Reduction of the cutting forces and tool wear as well as the improvement of the surface integrity of the machined surfaces [1-4] can be achieved when an ultrasonic vibration is applied to the cutting tool. These benefits make the UAT process a promising alternative for the machining of difficult-to-cut materials as Titanium alloys. Presently, the machining processes for these materials are limited to low material removal rates (MRR) trying to avoid excessive tool wear rates or cutting force values. Thus, the implementation of UAT based processes for the manufacturing of components on difficult-to-cut materials shows a great industrial potential.

In order to evaluate the industrial applicability of the UAT systems, the effects of the ultrasonic actuation on process outputs need to be adequately identified. In the case of the cutting force reductions generated during UAT processes, several sources have been identified to have the effect on them, as the intermittent cutting resulting from the ultrasonic vibration [1], the friction coefficient on the rake tool face [5, 4], the accelerations on the chip being generated during the vibration of the cutting tool [6] or the material yield stress reduction due to acoustic softening [7].

The present work follows an experimental approach for the characterization of the effect of the ultrasonic vibrations on the force reductions during the UAT process, in comparison to conventional turning. After testing the effect of the process for a wide range of parameters, empirical expressions are proposed for the calculation of the force reductions during UAT processes. Finally, the capabilities of these expressions to reproduce the experimental behaviour are discussed and evaluated.

10.1016/j.procir.2018.08.227

2. Ultrasonic assisted turning device

The UAT system is comprised of a 20 kHz ultrasonic transducer and booster from MPI Ultrasonics and a custom made sonotrode adapted to hold a cutting tool. It is designed to apply an ultrasonic vibration in the tangential (cutting speed) direction on the cutting tool. The ultrasonic transducer is actuated by a generator capable of modifying the amplitude output of the sonotrode. In order to evaluate the behavior of the UAT system, the vibration output at the tool tip was measured using of a Laser Doppler Vibrometer from Polytec (OGV-505 Sensor head + OFV-5000 controller). The obtained signals were acquired by a NI USB-6366 acquisition card, employing a sampling frequency of 2 MHz.

Figure 1 shows an example for an acquisitions and its power spectrum. On the right hand side of the figure, detailed views for the amplitude signal and the power spectrum are shown. As it can be seen, the system provides a high quality sinusoidal output at the tool tip, with a sole predominant frequency component at 20.445 kHz.

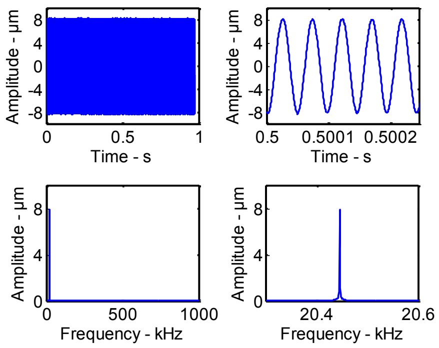

Fig. 1. System vibration measurement and power spectrum.

3. Experimental analysis of cutting force reductions

Experimental machining tests were carried out in order to evaluate the effect of the UAT process in comparison to conventional dry turning. Cylindrical turning tests were carried out on Ti6Al4V AMS4928 bars with CCMT 060204-MF 1115 carbide inserts from Sandvik. The UAT device was installed on a Danobat NA-150 lathe to perform cutting tests. In order to enable the measurement of the cutting forces generated during the machining tests, a three channel force dynamometer (Kistler 9129AA) was included on the clamping configuration for the UAT device (See Figure 2).

Some cutting parameters were modified during the cutting tests in order to analyze their effect on the forces generated during the UAT process (Table 1). The UAT process is controlled by the tool-workpiece contact ratio (TWCR) [1], which is the ratio of the tool-workpiece contact time (t_c) during a whole vibration period (T) as shown in (1). Thus, the parameters (V_c, a) affecting the TWCR were modified in order to analyze their effect. Also the effect of the parameters directly affecting the chip load (f_v, ap) and, thus, the force magnitude were analyzed. The tests were carried out with fresh tools to ensure that the measured cutting force values were not distorted by the appearance of tool wear.

$$TWCR = \frac{t_c}{T} \qquad (1)$$

Fig. 2. Image of the UAT system mounted on the lathe.

Table 1. Parameters analyzed during the cutting tests and their values

Parameter	Values
Cutting speed – V_c (m/min)	20-30-40-50-55
Feed per turn – f_v (mm/v)	0,1-0,2
Depth of cut – ap (mm)	0,1-0,2
Vibration frequency - f (kHz)	20,445
Vibration amplitude - a (µm)	0-8-10-12

Each cutting test was performed employing one value for the cutting speed, the feed rate and the depth of cut. In the case of the vibration amplitude, it was modified along the tests. Figure 3 shows the cutting forces (*Ft*: tangential force, *Fa*: axial force, *Fr*: Radial force) obtained for one of the tests. The effect of applying and increasing the vibration amplitude on the force components can be observed on the figure. Zone 1 corresponds to conventional cutting (a = 0 µm), while zones 2, 3 and 4 correspond to UAT with 8, 10 and 12 µm of vibration amplitude respectively.

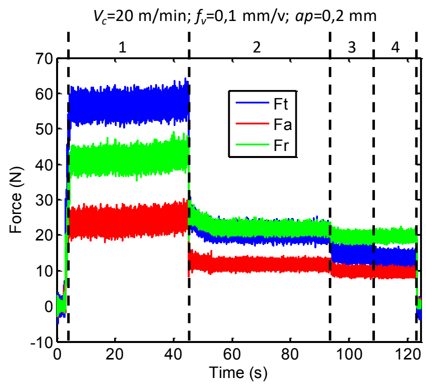

Fig. 3. Force measurements obtained for a cutting test.

4 repetitions were performed for each test in order to verify the repeatability of the obtained results. For each repetition, the reductions of the cutting forces when applying ultrasonic vibrations on the tool were calculated in comparison to values for conventional cutting. These reductions were obtained in percentage values following the expression (2). Then, mean reduction values and standard deviations were calculated for each test. The standard deviation obtained for the reduction of each force component was 4.76% for tangential force, 8.62% for axial force and 9.04% for radial force.

$$\%RF_i = 100 \cdot \frac{F_i^{Conv} - F_i^{UAT}}{F_i^{Conv}} \qquad (2)$$

Once obtained the percentage reductions for the three force components, the mean effect of the tested variables was obtained (Table 2). As it can be seen, the effect of the tool feed (f_v) and the depth of cut (ap) are lower than the standard deviations obtained for the reduction of each force component. Therefore it can be said that their effect on the force reductions is negligible. On the contrary, the cutting speed (V_c) and the vibration amplitude (a) show noteworthy effects on them. These effects agree qualitatively with results published scientific in bibliography [1, 3, 4, 8, 9].

Table 2. Effect of the tested parameters on force reductions

Parameter	*%RFt*	*%RFa*	*%RFr*
V_c	-26.55	-26.35	-38.43
f_v	-4.43	1.23	-0.53
ap	-2.17	3.74	-0.86
a	23.83	13.52	11.17

4. Empirical modeling

Once identified the parameters with significant effects on the reduction of the force components, an empirical modeling stage was carried out in order to obtain expressions that would allow the calculation of the force reductions when applying UAT in comparison to conventional turning. In the case of the tangential force, Figure 4 shows the graphical representation of the obtained percentage reduction values for this force component.

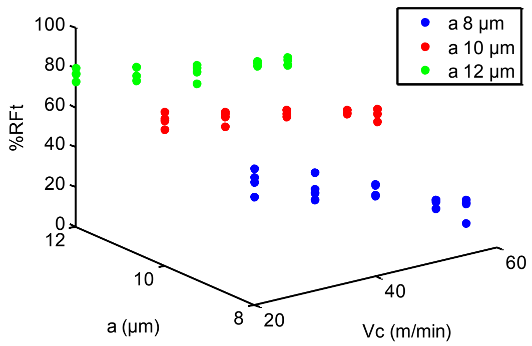

Fig. 4. Reductions obtained for the tangential force component.

As it can be seen, the tangential force reductions show a linear evolution with the cutting speed for the tested vibration amplitudes. Thus, a linear relationship was defined between the tangential force reduction and the cutting speed:

$$\%RF_t = p_1 \cdot V_c + p_2 \qquad (3)$$

In order to include the effect of the vibration amplitude on the evolution of the tangential force reduction, it was assumed that the constant parameters p_1 and p_2 from (3) are lineally dependent on the vibration amplitude:

$$p_j = c_{j1} \cdot a + c_{j2} \qquad (4)$$

This way, by combining equations (3) and (4), we obtain the expression (4) for the force reductions on the tangential component. The value for the parameters C_{ij} from equation (5) were obtained by conducting a linear least squares fitting of this expression to the experimental results obtained for the tangential force component. The obtained values are exposed in Table 3 and Figure 5 shows a graphical representation of the obtained fitting surface together with the experimental results.

$$\%RF_t = c_{11} \cdot V_c \cdot a + c_{12} \cdot V_c + c_{21} \cdot a + c_{22} \qquad (5)$$

Table 3. Values for the parameters from eq. (4)

Parameter	*%RFt*
C_{11}	0.1423
C_{12}	-2.1213
C_{21}	0.6219
C_{22}	79.7539

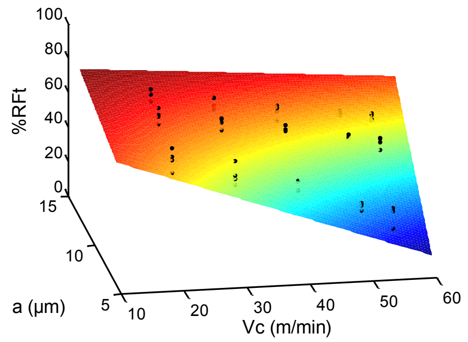

Fig. 5. Fitting surface obtained for the tangential force component.

In the case of the axial and radial force components, the evolution of their reduction with the cutting speed does not show a linear shape. Instead, their evolution shows a curved shape as it can be seen on Figure 6 for the case of the radial force component. This way, a quadratic relationship was defined between the reduction of the axial and radial force components and the cutting speed (6). As in the case of the tangential force component, a linear relationship as (4) was assumed between the vibration amplitude and the parameters p_1, p_2 and p_3 from (6). Thus, the expression for the force reduction in the axial and the radial direction would be (7).

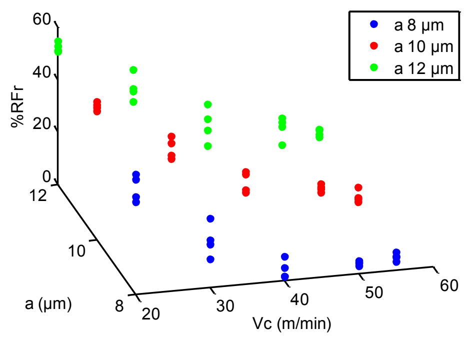

Fig. 6. Reductions obtained for the radial force component.

$$\%RF_{a,r} = p_1 \cdot V_c^2 + p_2 \cdot V_c + p_3 \qquad (6)$$

$$\%RF_{a,r} = c_{11} \cdot V_c^2 \cdot a + c_{12} \cdot V_c^2 + c_{21} \cdot V_c \cdot a + c_{22} \cdot V_c + c_{31} \cdot a + c_{32} \qquad (7)$$

After a linear least squares fitting procedure, the obtained parameters C_{ij} from equation (7) can be seen in Table 4 for both axial and radial force components. The fitting surface generated when introducing the parameters from Table 4 in the expression (7) can be seen in Figure 7 for the case of the radial force component.

Table 4. Values for the parameters from eq. (6).

Parameter	*%RFa*	*%RFr*
C_{11}	0.0011	-0.0054
C_{12}	0.0004	0.0892
C_{21}	-0.0837	0.3503
C_{22}	-0.7484	-7.3262
C_{31}	4.8987	-1.7281
C_{32}	31.7239	128.8476

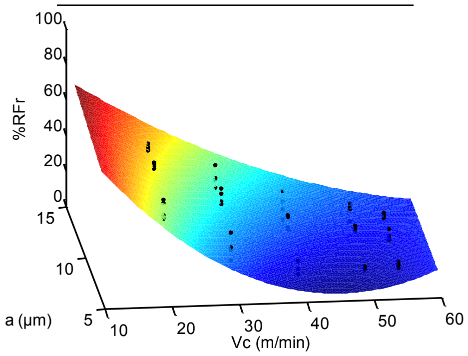

Fig. 7. Fitting surface obtained for the radial force component.

5. Discussion

The present work analyses a broad range for the process parameters with the highest effect on the cutting forces obtained during turning in order to enable the development of a predictive model for the force reductions during UAT. Besides the effect of the contact ratio reduction generated by the ultrasonic vibrations, no simple expression was found in bibliography for estimating the force reductions during UAT processes. This way, the results obtained from the empirical expressions generated in the present work were compared to the ones coming from the contact ratio variation (8):

$$\%RF_i = 100 \cdot (1 - TWCR) \quad (8)$$

Table 5 shows the values concerning the correlation coefficient (R^2), the mean error (ME) and the root squared mean error (RSME) for both models in comparison to the experimental results. As it can be seen, the TWCR model obtains close results to the performed experimental tests for the tangential force component, while the differences obtained for the axial and radial components are noteworthy.

In the case of the empirical expressions obtained on the present work, the results show a very good agreement to the experimental tests. With null mean errors, all the RMSE values are below the experimental standard deviation (σ_{exp}) values for each force component and the correlation coefficients are above 0.9, except for the axial component.

Table 5. Evaluation of results from present model and TWCR

Component	σ_{exp}	Model	R^2	ME	RMSE
%RFt	4.76%	Present	0.92	1e-15	4.17
		TWCR	0.87	-7.68	9.40
%RFa	8.62%	Present	0.83	7e-15	4.83
		TWCR	0.79	11.34	13.37
%RFr	9.04%	Present	0.95	4e-14	3.75
		TWCR	0.73	27.78	29.07

6. Conclusions

Next conclusions can be drawn from the results obtained during this work:

- The chip load (f_v, *ap*) has a negligible effect on the force reductions generated by the UAT process.
- The parameters found to have a significant effect in these force reductions are the ones affecting the TWCR (V_c, *a*).
- It was possible to define empirical expressions that allow calculating the effect of the UAT process concerning force reductions with a very good degree of accuracy.
- The physical variables affecting the reduction of axial and radial force components need to be analyzed in detail besides purely kinematic parameters (V_c, *a*).

The empirical expressions exposed on the present work can help on the validation of analytical and numerical models for the UAT process. Further work shall be carried out with UAT models for analyzing the physical sources affecting the force modifications generated by the UAT process.

References

[1] Nath C, Rahman M. Effect of machining parameters in ultrasonic vibration cutting. Int J Mach Tools Manuf 2008; 48: 965–974.
[2] Maurotto A, Muhammad R, Roy A, Silberschmidt VV. Enhanced ultrasonically assisted turning of a β-titanium alloy. Ultrasonics 2013; 53: 1242–1250.
[3] Muhammad R, Hussain MS, Maurotto A, Siemers C, Roy A, Silberschmidt VV. Analysis of a free machining α+β titanium alloy using conventional and ultrasonically assisted turning. J Mater Process Tech Vol. 214, 2014, p. 906–915.
[4] Patil S, Joshi S, Tewari A, Joshi SS. Modelling and simulation of effect of ultrasonic vibrations on machining of Ti6Al4V. Ultrasonics 2014; 54: 694–705.
[5] Mitrofanov AV, Ahmed N, Babitsky VI, Silberschmidt VV. Effect of lubrication and cutting parameters on ultrasonically assisted turning of Inconel 718. J Mater Process Technol 2005; 162–163: 649–654.
[6] Razavi H, Nategh MJ, Abdullah A. Analytical modeling and experimental investigation of ultrasonic-vibration assisted oblique turning, part II: Dynamics analysis. Int J Mech Sci 2012; 63: 12–25.
[7] Verma GC, Pandey PM, Dixit US. Modeling of static machining force in axial ultrasonic-vibration assisted milling considering acoustic softening. Int J Mech Sci 2018; 136: 1–16.
[8] Muhammad R, Maurotto A, Demiral M, Roy A, Silberschmidt VV. Thermally enhanced ultrasonically assisted machining of Ti alloy. CIRP J Manuf Sci Technol 2014; 7: 159–167.
[9] Razavi H., Nategh MJ, Abdullah A. Analytical modeling and experimental investigation of ultrasonic-vibration assisted oblique turning, part III: Experimental investigation. Int J Mech Sci 2012; 63: 26–36.